Highly Anisotropic Magnon Dispersion in Ca_2RuO_4: Evidence for Strong Spin Orbit Coupling

S. Kunkemöller,[1] D. Khomskii,[1] P. Steffens,[2] A. Piovano,[2] A. A. Nugroho,[3] and M. Braden[1,*]
[1]*II. Physikalisches Institut, Universität zu Köln, Zülpicher Str. 77, D-50937 Köln, Germany*
[2]*Institut Laue Langevin, 6 Rue Jules Horowitz BP 156, F-38042 Grenoble CEDEX 9, France*
[3]*Faculty of Mathematics and Natural Sciences, Institut Teknologi Bandung, Jl. Ganesha 10, Bandung 40132, Indonesia*
(Received 23 July 2015; published 8 December 2015)

The magnon dispersion in Ca_2RuO_4 has been determined by inelastic neutron scattering on single crytals containing 1% of Ti. The dispersion is well described by a conventional Heisenberg model suggesting a local moment model with nearest neighbor interaction of $J = 8$ meV. Nearest and next-nearest neighbor interaction as well as interlayer coupling parameters are required to properly describe the entire dispersion. Spin-orbit coupling induces a very large anisotropy gap in the magnetic excitations in apparent contrast with a simple planar magnetic model. Orbital ordering breaking tetragonal symmetry, and strong spin-orbit coupling can thus be identified as important factors in this system.

DOI: 10.1103/PhysRevLett.115.247201 PACS numbers: 75.30.Ds, 75.25.-j, 75.30.Et, 75.50.Ee

The properties of strongly correlated systems with significant spin-orbit coupling (SOC) present a challenging problem. For most $3d$ transition-metal compounds one can treat SOC as a weak perturbation. It leads to single-site and exchange magnetic anisotropy, possibly to an antisymmetric (Dzyaloshinskii-Moriya) exchange, and it largely determines the magnetoelastic coupling and magnetostriction. The situation can be different in case of strong SOC, which causes novel phenomena such as the anomalous Hall effect [1], the spin Hall effect [2], and topological insulators [3,4]. Strong SOC is able to change the character of the multiplet state of the corresponding ions, which is intensively studied for the case of the reduction of the magnetic state of Ir^{4+} (electronic structure $5d^5$ or t_{2g}^5, $L_{\mathrm{eff}} = 1$, $S = 1/2$) to an effective Kramers doublet with $j = 1/2$ [5]. But even more drastic effects can be expected for heavy ions with d^4 occupation (t_{2g}^4, $L_{\mathrm{eff}} = 1$, $S = 1$), e.g., in Ir^{5+}, Ru^{4+}, Os^{4+}, etc. [6]. According to Hund's rules (generalized for ions sensing crystal electric fields) the ground state should be a nonmagnetic singlet with $j = 0$; see, e.g., Refs. [7,8]. And, indeed, isolated Ir^{5+} ions and also most of the concentrated Ir^{5+} compounds are nonmagnetic, although a few magnetic Ir^{5+} cases are known [9]. In a solid, magnetic order can occur even if the ground state of an isolated ion is a singlet, see Chap. 5.5 in Ref. [8], but it requires a strong exchange interaction, so that the exchange splitting of excited magnetic states (in the Ru^{4+} case a $j = 1$ triplet) is larger than the energy difference between the ground-state singlet and the excited triplet, which is given by the SOC parameter λ. The SOC can also be at least partially suppressed by a noncubic crystal field (CF), Δ_{noncub}, which splits the t_{2g} ($L_{\mathrm{eff}} = 1$) triplet and stabilizes real orbitals. Both these factors, CF and magnetic interaction, can combine to suppress the $j = 0$ state and to eventually induce the magnetically ordered ground state. In terms of energy scales, one should expect such magnetic ordering for $\Delta_{\mathrm{noncub}} + \mu H_{\mathrm{exch}} > \lambda$, which seems quite unlikely for Ir^{5+}, where $\lambda = (\zeta/2S) = \zeta/2$ amounts to 0.2 to 0.25 eV (ζ is the atomic spin-orbit parameter). But for $4d$ compounds this relation can easily be reached, as for Ru^{4+} $\lambda \sim 0.075$ eV [6,10]. Indeed, practically all Ru^{4+} compounds order magnetically aside from the metallic ones—and even some metallic ruthenates are magnetic, such as the ferromagnetic metal $SrRuO_3$. The persisting role of SOC in these magnetic Ru^{4+} compounds is an intriguing open issue.

Ca_2RuO_4 (CRO) is such a Ru^{4+} case, which has been intensively studied as the Mott-insulating analogue of the unconventional superconductor Sr_2RuO_4 [11–14]. CRO exhibits a metal-insulator (MI) transition at 357 K, which is accompanied by a flattening of the RuO_6 octahedra [13–16]. This flattening continues upon further cooling until it saturates near the onset of magnetic order at $T_N \sim 110$ K. The magnetic structure is antiferromagnetic (AFM) with moments aligned parallel to the layers [13,16]; see Fig. 1(a). The electronic structure has been studied by various approaches [17–21]. From the spectroscopic study of CRO it was concluded that SOC indeed plays an important role but is not sufficiently strong to stabilize the $j = 0$ state [17]. Density functional theory calculations indicate a pronounced shift in orbital polarization leading to almost full electron occupation of the d_{xy} levels at low temperature [18–22]. More recently, the $j = 0$ state was explicitly proposed for CRO [6,10]. Starting from the scenario of strong SOC and including noncubic CF and intersite exchange, the magnetically ordered state in CRO is reproduced and several unusual features of the magnetic excitation spectrum of CRO are predicted, such as a peculiar shape and large width. The alternative, more conventional picture is to attribute the magnetism of

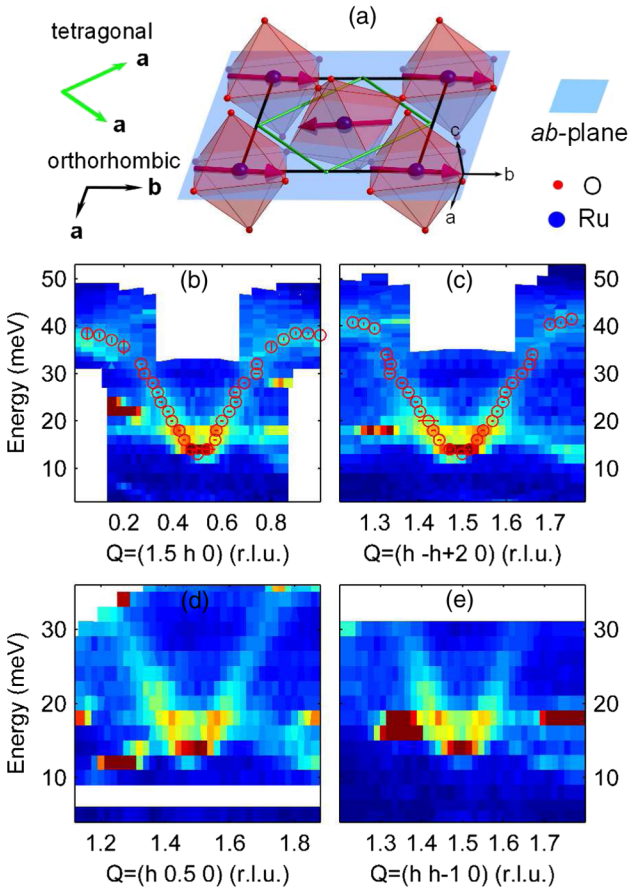

FIG. 1 (color online). (a) Sketch of the magnetic and crystal structure of CRO; only a single layer of RuO_6 octahedra is shown (Ru in blue balls, O in small red points) including the tetragonal and larger orthorhombic cells. Note that magnetic moments are slightly canted (by about 6 degrees) resulting in a weak ferromagnetic component in such a single layer [13]. The small arrows added at the tip of the rightmost moment indicate the polarization of the two transversal and the longitudinal modes. (b)–(e) Intensity distribution in energy versus scattering vector $\mathbf{Q}$ planes taken at 2 K around the (1.5 0.5 0) magnetic zone center. (b) and (d) The symmetrically equivalent dispersion along the $(0, \xi, 0)$ and $(\xi, 0, 0)$ directions, subplot (c) and (e) along $(\xi, \xi, 0)$ and $(\xi, -\xi, 0)$. The color coding corresponds to the raw data. Open symbols indicate the dispersion obtained by fitting single scans. Data were taken on IN8 with final energies of 35 meV for constant $\mathbf{Q}$ scans at high energy transfer and 14.7 meV elsewhere.

CRO to the conventional $S \sim 1$ state of Ru^{4+} ions, with SOC playing a less significant but still prominent role. In this case one can describe the magnetic state, including spin waves, by the usual exchange Hamiltonian.

Here we present an inelastic neutron scattering (INS) study and spin-wave calculations of the magnetic excitations in CRO. Details of the INS experiments and on the sample characterization of the crystals containing 1% of Ti are given in the Supplemental Material [23]. We find that a conventional model can well describe the obtained dispersion, while there are considerable differences with the proposed $j = 0$ model [10]. Most interestingly, there is a sizable spin gap which indicates that rotating the magnetic moment within the layers costs large energy. The breaking of the local tetragonal symmetry and the associated orbital polarization, which has been neglected in theory so far [18–22], are important parameters to understand the magnetism in CRO.

Figures 1(b)–1(e) show color mappings of the measured intensity distribution. Because of the weakness of scattering in CRO (small moment and rapidly decreasing form factor) contaminations by various phonon branches are highly visible. By analyzing and comparing results taken in different Brillouin zones and geometries the dispersion can be unambiguously determined. Magnon excitations start at the AFM Bragg points $((2n_h + 1)/2\ (2n_k + 1)/2\ n_l)$ with integer n_h, n_k, and n_l. However, there is a sizable spin gap of 13.04(5) meV. For a square planar antiferromagnet the magnon dispersion extends from $\mathbf{Q} = (0.5\,0.5)$ to (0.75 0.75) in the [1 1] direction, as (1 1) is a Bragg point, and to (0 0.5) in the [1 0] direction. $\mathbf{Q} = (0.25\,0.25)$ and (0 0.5) are AFM Brillouin zone boundaries. In CRO there is, however, a severe structural distortion [16]. Some characteristic scans performed to determine the magnon dispersion in CRO are shown in Fig. 2. Constant energy scans at intermediate energy cut through the magnon cones at two positions. Constant $\mathbf{Q}$ scans taken

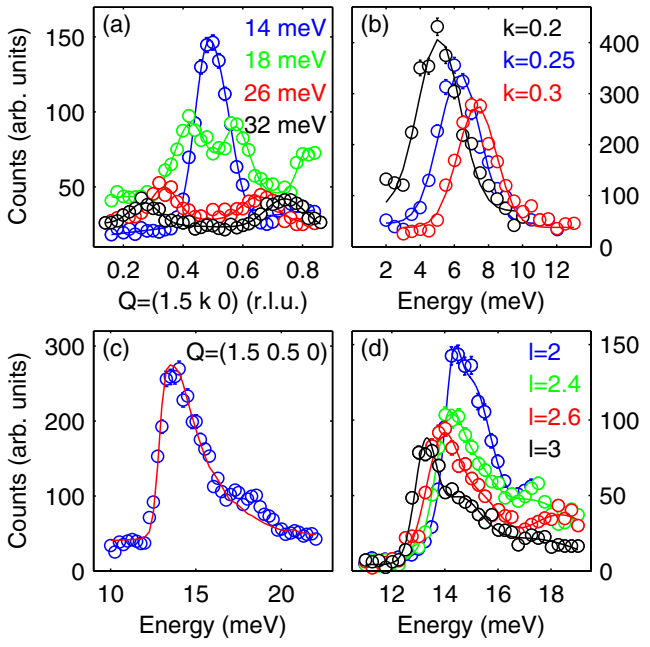

FIG. 2 (color online). Several characteristic scans taken at 2 K on IN8: (a) Constant energy scans at (1.5, k, 0) fitted with Gaussians and background. (b) Phonon scans taken at $\mathbf{Q} = (\xi, 2, 0)$; the lines correspond to the folding of the resolution function with a simple linear phonon dispersion. No additional parameter is needed to describe the shape of the intensity profile. (c) and (d) Energy scans at the zone center (1.5 0.5 0) and at (0.5 0.5 l).

just at the AFM zone center show a characteristic asymmetric shape, see Figs. 2(c) and 2(d): Intensity rapidly increases when crossing the spin gap and slowly diminishes with further energy increase. We have calculated the folding of the spin-wave dispersion including its expected signal strength with the experimental resolution using the RESLIB [24] package and verified that scans across transversal acoustic phonons are well reproduced; see Fig. 2(b). The steep spin wave dispersion perfectly describes the asymmetric shape of the spectra taken at the zone center; see Fig. 2(c). The total width of the dispersion is low, as maximum energies of 37.8(3) and 41.2(5) meV are reached at the magnetic zone boundaries, (0.5 0 0) and (0.25 0.25 0).

In order to describe the magnon dispersion we use a conventional Heisenberg equation: $H = \sum_{\mathbf{i},\mathbf{j}} J_{i,j} \mathbf{S_i} \cdot \mathbf{S_j} - \delta \sum_i (S_i^y)^2$. We include a single-site anisotropy term arising from SOC but note that anisotropic exchange parameters would lead to similar results. The model for fully dominant SOC is presented in Ref. [10]. We set $S = 0.67$ following the neutron diffraction study [13]. The sum runs over pairs of magnetic ions, so that each pair or bond appears twice. Spin waves were calculated with the Holstein-Primakoff transformation as described in Refs. [25,26]. We include the nearest-neighbor magnetic exchange of $J = 8$ meV, next-nearest neighbor interaction along the orthorhombic a and b directions of $J_{nna} = J_{nnb} = 0.7$ meV, and an AFM coupling between neighboring layers. The next-nearest neighbor interaction is chosen isotropic, as the twinned crystal used in the (1 0 0)/(0 1 0) geometry prohibits distinguishing these directions. The need for the additional parameter can be seen when comparing the magnon energies at $\mathbf{q} = (0.25\,0.25\,0)$ and (0.5 0 0), which are identical in the model with only nearest-neighbor interaction. The interlayer coupling, $J_c = 0.03$ meV is the only parameter that breaks the tetragonal symmetry in our model aside from the single-ion anisotropy. Note, however, that the crystal structure is orthorhombic, lifting the degeneracy of magnetic interaction parameters. We chose the AFM interaction between the Ru at (0,0,0) and that at (0,0.5,0.5) (in the orthorhombic cell [13]), which stabilizes an A centered magnetic structure with magnetic space group Pbca [16].

The magnetic moment in CRO points along the orthorhombic b direction; see Fig. 1(a). Therefore, one might expect a large gap for the magnetic excitations involving rotations of the moment out of the RuO_2 layers, and much softer in-plane modes. The latter are described by the expectedly small in-plane anisotropy. Following Refs. [26,27] both branches can be described simultaneously with two anisotropy parameters. Surprisingly, in CRO the in-plane anisotropy turned out to be extremely strong. The magnon dispersion starts at 13.04(5) meV, which we may identify with the in-plane gap. There is no magnon branch at lower energy as is clearly shown in the intensity maps, although there is a weak localized feature observed at 5 meV close to the magnetic zone boundary [23]. As shown in Figs. 2(d) and 3 there is a finite interlayer dispersion visible in the scans taken at $\mathbf{Q} = (0.5\,0.5\,q_l)$ with the second untwinned crystal. The tetragonal [110] direction corresponds to orthorhombic b in the used mounting and thus to the direction of the magnetic moment; therefore, the transverse magnon with in-plane polarization (thus parallel to orthorhombic a) fully contributes. Also, in the other configuration there is a clear difference in spectra taken at $\mathbf{Q} = (0.5\,0.5\,0)$ and $= (1.5\,0.5\,0)$. For the twinned sample we superpose AFM zone centers and zone boundaries, and c polarized magnons will always contribute, while for the in-plane magnon the geometry condition that only magnetic components perpendicular to $\mathbf{Q}$ contribute, suppresses some modes. The fact that we see a clear difference at various $((2n_h+1)/2\ (2n_k+1)/2\ n_l)$ unambiguously shows that the modes dispersing between 13.04(5) and 14.2(1) meV possess an in-plane polarization. This furthermore agrees with the Q_l dependence of the signal. We may thus conclude that the lowest magnon branch in CRO possesses an in-plane character and that it disperses between 13.04(5) and 14.2(1) meV along the c direction and up to 41.2 and 37.8 meV along the $(\xi\,\xi\,0)$ and $(\xi\,0\,0)$ paths, respectively. We cannot identify the c polarized modes, as they may remain hidden in the asymmetric shape or even lie at much higher energy. There is some evidence for a nearly flat branch around 36 meV, but we cannot fully rule out that these modes are purely nuclear or that they carry longitudinal polarization. For simplicity, the experimental dispersion is described by an easy-axis anisotropy [27]; see Fig. 3.

The magnon dispersion including its large gap can be very well described within the spin-wave theory, suggesting a conventional local moment $S \sim 1$ magnetism with a strong—but not decisive—impact of SOC. Starting from the other scenario, a spin-orbit driven $j = 0$ singlet nature which is rendered magnetic by

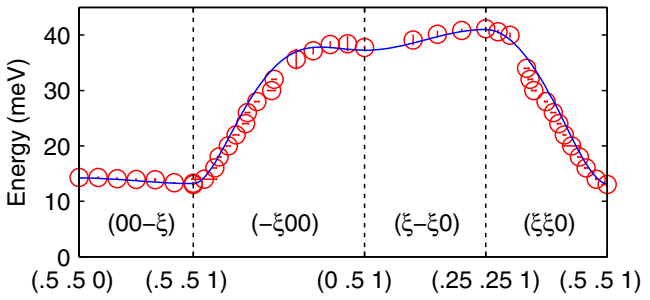

FIG. 3 (color online). Dispersion of the magnon branch along the main symmetry directions at $T = 2$ K. The open symbols indicate the values obtained by fitting the raw data scans with Gaussians or by folding the resolution function with the modeled dispersion. Lines correspond to the spin-wave calculations with the Heisenberg model as described in the text.

noncubic CF and intersite exchange, Akbari and Khaliullin [10] predicted several unusual features of the magnetic excitation spectrum, such as the energy continuously softening from the value λ at Γ, and the presence of extra modes in some part of the spectrum. Our results, however, do not support this model [10]. First, the observed dispersion is much flatter than this prediction, as it does not reach energies of the order of the expectedly large values of λ, and as there is a strong gap. Second, the singlet picture predicts a continuously increasing dispersion near the AFM zone boundaries, while our experiments find the saturation predicted by the Heisenberg model; see Figs. 1 and 2. The Heisenberg scenario also implies several branches: two transversal branches arise from the orthorhombic anisotropy [in-plane and c polarized, see Fig. 1(a)], and longitudinal modes can exist in CRO, which the small ordered moment and the closeness of the MI transition suggest being near the border to itinerancy.

Using the standard description, with the hopping parameters $t \sim 100$ meV, obtained by *ab initio* calculations [28,29], and using the Hubbard's $U \sim 2$ eV, we would obtain for the exchange constant $J = 2t^2/U \sim 10$ meV, in good agreement with our experimental finding. However, CRO is not a strong Mott insulator with completely localized electrons as it is already indicated by the low-lying MI transition. In this case, the basic $j = 0$ ansatz may not be a good starting point, as the $j = 0$ state can be suppressed by electron hopping. Also for Ir^{4+} (specifically for Na_2IrO_3) the sizable hopping modifies the whole picture [30,31], leading to novel quasimolecular orbital states with reduced impact of SOC. The conspicuous but typical absence of $j = 0$ physics in most of the Ru^{4+} materials seems largely connected with the hopping.

Another argument in favor of the applicability of the usual picture of Ru^{4+} ions ($S \sim 1$) is the strong flattening of RuO_6 octahedra [13,15] occurring below the MI transition. Such distortion is typical for the usual Jahn-Teller effect: it stabilizes the electron doubly occupied d_{xy} orbital, leaving two electrons on d_{xz} and d_{yz}. In such a state the orbital moment and spin-orbit interaction are partially quenched. The sign of this distortion proves that in this system the Jahn-Teller effect is stronger than the SOC, which would have caused the opposite distortion and CF splitting [8]. Recent spectroscopy data [21] confirm this significant splitting of t_{2g} orbitals.

On the other hand, the observation of the strong in-plane magnetic gap is remarkable for a layered system. It underlines the relevance of the SOC in CRO even in the conventional scenario. Several Raman scattering experiments observed an additional signal in B_{1g} symmetry appearing in the AFM phase [32–34]. This feature was interpreted as a two-magnon excitation, but our results clearly rule out such explanation. The Raman feature appears at 102 $cm^{-1} = 12.6$ meV at 10 K, which is much below the energies for two magnon excitations and the expected peak in the two-magnon density of states (near 80 meV). Instead, this energy is very close to that of the in-plane gap mode in our sample containing 1% of Ti. The single magnon mode, however, is not Raman active in first approximation, demanding further analysis. The temperature dependence and the extreme broadening of the Raman signal at higher temperature agree reasonably well with the corresponding behavior of the magnon gap; see inset in Fig. 4(b).

The magnetic in-plane anisotropy in CRO must originate from SOC and from an orbital arrangement breaking tetragonal symmetry. There have been many experimental and theoretical analyses [17–22] elucidating the change of the orbital polarization upon cooling and the increasing electron occupation of the d_{xy} versus the d_{xz}/d_{yz} orbitals following the flattening of the RuO_6 octahedron. This distortion possesses E_g symmetry, which is the most frequently analyzed in Jahn-Teller models [35]. The t_{2g} orbitals, however, also couple to the T_{2g} octahedron distortions [35] which break tetragonal symmetry in the case of CRO but which were neglected so far. The temperature dependence of the crystal structure of CRO in the insulating phase reveals an ongoing elongation of the RuO_6 octahedra [13,15] along the orthorhombic b direction along which moments align. This distortion corresponds to the T_{2g} "scissor" mode of the free octahedron [35] lifting the d_{xz}/d_{yz} degeneracy. Similar to a tetragonal distortion, e.g., along the z axis, which would stabilize electron orbitals with $l^z = \pm 1$, $(d_{xz} \pm id_{yz})$, and which, by SOC would orient spins along the z direction, (or a trigonal elongation along [111] (in cubic setting), which would make [111] an easy axis, see, e.g., Ref. [8], such T_{2g} distortion (elongation along the b axis) makes the orthorhombic b direction the easy axis.

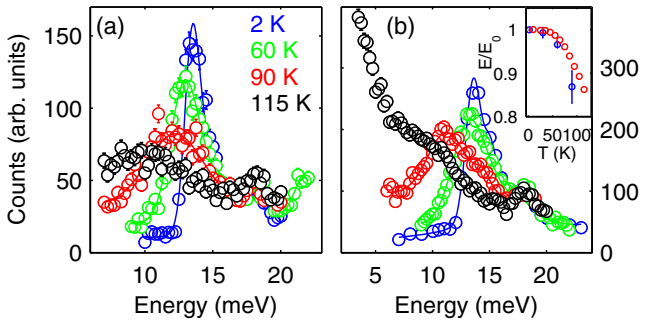

FIG. 4 (color online). Temperature dependence of the magnetic scattering at the AFM zone center (1.5,0.5,0) measured on IN8 with the Si monochromator and $k_F = 1.97$ (a) and 2.662 $Å^{-1}$ (b) The sharp peak associated with the in-plane spin gap mode softens and broadens considerably. The inset shows the energy of the spin gap scaled to its low temperature value (blue) compared to that of a Raman signal taken from Ref. [34] (red). Note that the Raman data were taken on pure Ca_2RuO_4, while our sample contains 1% of Ti.

In conclusion, we have studied the magnon dispersion in CRO, which considerably differs from recent predictions for a $j = 0$ singlet ground state. Instead, the dispersion is well described in a local moment Heisenberg model with strong anisotropy terms yielding a nearest-neighbor exchange interaction of $J = 8$ meV, which agrees with the large calculated hopping integrals. Large hopping seems to be the main cause for the suppression of the $j = 0$ state in Ru^{4+} compounds. On the other hand, the remarkably strong in-plane anisotropy clearly shows that considering tetragonal crystal fields is insufficient. There is important orbital polarization breaking tetragonal symmetry, which is related to the prominent elongation of RuO_6 octahedra along the orthorhombic b direction and which renders spin-orbit coupling still active in this system.

Part of this work was supported by the Institutional Strategy of the University of Cologne within the German Excellence Initiative and by Deutsche Forschungsgemeinschaft through Project FOR 1346. We acknowledge stimulating discussions with M. Grüninger, G. Khaliullin, P. van Loosdrecht, and T. Lorenz.

Note added.—After completion of this work we became aware of similar inelastic neutron scattering and theoretical analysis of magnetic excitations in Ca_2RuO_4 [36]. The reported dispersion of the in-plane transverse branch fully agrees with our observations. Jain *et al.* propose a model of an effective $S = 1$ state with strong anisotropy arising from spin-orbit coupling included, which is similar to the interpretation given here.

*braden@ph2.uni-koeln.de

[1] N. Nagaosa, J. Sinova, S. Onoda, A. H. MacDonald, and N. P. Ong, Rev. Mod. Phys. **82**, 1539 (2010).
[2] A. Shitade, H. Katsura, J. Kunes, X.-L. Qi, S.-C. Zhang, and N. Nagaosa, Phys. Rev. Lett. **102**, 256403 (2009).
[3] M. Z. Hasan and C. L. Kane, Rev. Mod. Phys. **82**, 3045 (2010).
[4] X. L. Xi and S. C. Zhang, Rev. Mod. Phys. **83**, 1057 (2011).
[5] D. Pesin and L. Balents, Nat. Phys. **6**, 376 (2010); W. Witczak-Krempa, G. Chen, Y. B. Kim, and L. Balents, Annu. Rev. Condens. Matter Phys. **5**, 57 (2014).
[6] G. Khaliullin, Phys. Rev. Lett. **111**, 197201 (2013).
[7] A. Abragam and B. Bleaney, *Electron Paramagnetic Resonance of Transition Ions* (Clarendon Press, Oxford, 1970).
[8] D. I. Khomskii, *Transition Metal Compounds* (Cambridge University Press, Cambridge, England, 2014).
[9] G. Cao, T. F. Qi, L. Li, J. Terzic, S. J. Yuan, L. E. DeLong, G. Murthy, and R. K. Kaul, Phys. Rev. Lett. **112**, 056402 (2014).
[10] A. Akbari and G. Khaliullin, Phys. Rev. B **90**, 035137 (2014).
[11] S. Nakatsuji and Y. Maeno, Phys. Rev. Lett. **84**, 2666 (2000); S. Nakatsuji and Y. Maeno, J. Solid State Chem. **156**, 26 (2001).
[12] G. Cao, S. McCall, M. Shepard, J. E. Crow, and R. P. Guertin, Phys. Rev. B **56**, R2916 (1997).
[13] M. Braden, G. André, S. Nakatsuji, and Y. Maeno, Phys. Rev. B **58**, 847 (1998).
[14] C. S. Alexander, G. Cao, V. Dobrosavljevic, S. McCall, J. E. Crow, E. Lochner, and R. P. Guertin, Phys. Rev. B **60**, R8422 (1999).
[15] O. Friedt, M. Braden, G. André, P. Adelmann, S. Nakatsuji, and Y. Maeno, Phys. Rev. B **63**, 174432 (2001).
[16] CRO crystallizes in space group Pbca with lattice constants $a = 5.39$, $b = 5.63$, and $c \approx 12$ Å. We use the tetragonal lattice in space group I4/mmm with $a = b \approx 3.9$ Å and $c \approx 12$ Å in accordance with most publications. Spin-wave calculations were performed in the orthorhombic cell and transformed to the tetragonal one.
[17] T. Mizokawa, L. H. Tjeng, G. A. Sawatzky, G. Ghiringhelli, O. Tjernberg, N. B. Brookes, H. Fukazawa, S. Nakatsuji, and Y. Maeno, Phys. Rev. Lett. **87**, 077202 (2001).
[18] A. Liebsch and H. Ishida, Phys. Rev. Lett. **98**, 216403 (2007).
[19] Z. Fang, N. Nagaosa, and K. Terakura, Phys. Rev. B **69**, 045116 (2004); Z. Fang and K. Terakura, Phys. Rev. B **64**, 020509(R) (2001).
[20] E. Gorelov, M. Karolak, T. O. Wehling, F. Lechermann, A. I. Lichtenstein, and E. Pavarini, Phys. Rev. Lett. **104**, 226401 (2010).
[21] C. G. Fatuzzo, M. Dantz, S. Fatale, P. Olalde-Velasco, N. E. Shaik, B. Dalla Piazza, S. Toth, J. Pelliciari, R. Fittipaldi, A. Vecchione, N. Kikugawa, J. S. Brooks, H. M. Ronnow, M. Grioni, Ch. Rüegg, T. Schmitt, and J. Chang, Phys. Rev. B **91**, 155104 (2015).
[22] V. I. Anisimov, I. A. Nekrasov, D. E. Kondakov, T. M. Rice, and M. Sigrist, Eur. Phys. J. B **25**, 191 (2002).
[23] See Supplemental Material at http://link.aps.org/supplemental/10.1103/PhysRevLett.115.247201 for the experimental details of the INS experiments and concerning the observation of an additional feature at low energy.
[24] A. Zheludev, *RESLIB 3.4c* (Oak Ridge National Laboratory, Oak Ridge, TN, 2007).
[25] Albert W. Sáenz, Phys. Rev. **125**, 1940 (1962).
[26] M. P. H. Thurlings, E. Frikkee, and H. W. de Wijn, Phys. Rev. B **25**, 4750 (1982).
[27] N. Qureshi, P. Steffens, S. Wurmehl, S. Aswartham, B. Büchner, and M. Braden, Phys. Rev. B **86**, 060410 (2012).
[28] H. Isobe and N. Nagaosa, Phys. Rev. B **90**, 115122 (2014).
[29] O. N. Meetei, W. S. Cole, M. Randeria, and N. Trivedi, Phys. Rev. B **91**, 054412 (2015).
[30] I. I. Mazin, S. Manni, K. Foyevtsova, H. O. Jeschke, P. Gegenwart, and R. Valentí, Phys. Rev. B **88**, 035115 (2013).
[31] K. Foyevtsova, H. O. Jeschke, I. I. Mazin, D. I. Khomskii, and R. Valentí, Phys. Rev. B **88**, 035107 (2013).
[32] C. S. Snow, S. L. Cooper, G. Cao, J. E. Crow, H. Fukazawa, S. Nakatsuji, and Y. Maeno, Phys. Rev. Lett. **89**, 226401 (2002).
[33] J. H. Jung, Solid State Commun. **133**, 103 (2005).
[34] H. Rho, S. L. Cooper, S. Nakatsuji, H. Fukazawa, and Y. Maeno, Phys. Rev. B **71**, 245121 (2005).
[35] I. B. Bersuker, *The Jahn-Teller Effect* (Cambridge University Press, Cambridge, England, 2006).
[36] A. Jain *et al.*, arXiv:1510.07011.